FocusChat: Text-guided Long Video Understanding via Spatiotemporal Information Filtering

Zheng Cheng, Rendong Wang, Zhicheng Wang

YITION.AI

{*zheng.cheng, rendong.wang, zhicheng.wang*}*@yition.ai*

Abstract

Recently, multi-modal large language models have made significant progress. However, visual information lacking of guidance from the user's intention may lead to redundant computation and involve unnecessary visual noise, especially in long, untrimmed videos. To address this issue, we propose FocusChat, a text-guided multi-modal large language model (LLM) that emphasizes visual information correlated to the user's prompt. In detail, Our model first undergoes the semantic extraction module, which comprises a visual semantic branch and a text semantic branch to extract image and text semantics, respectively. The two branches are combined using the Spatial-Temporal Filtering Module (STFM). STFM enables explicit spatial-level information filtering and implicit temporal-level feature filtering, ensuring that the visual tokens are closely aligned with the user's query. It lowers the essential number of visual tokens inputted into the LLM. FocusChat significantly outperforms Video-LLaMA in zero-shot experiments, using an order of magnitude less training data with only 16 visual tokens occupied. It achieves results comparable to the state-of-the-art in few-shot experiments, with only 0.72M pre-training data.

1. Introduction

Large Language Models (LLMs) [8, 10, 49] have emerged as powerful tools in the realm of natural language processing, achieving substantial success through extensive pre-training on vast amounts of textual data. Notable examples include GPT [36] and LLaMA [49, 50], which excel in generative and discriminative tasks within a cohesive framework. Recently, there has been an increasing trend in applying LLMs to multimodal tasks, highlighting their potential in areas such as image captioning [31, 35, 43] and question-answering [7, 18, 24, 32, 45, 71] that utilize various visual inputs. However, understanding long videos poses unique challenges [56, 62], especially in answering questions about
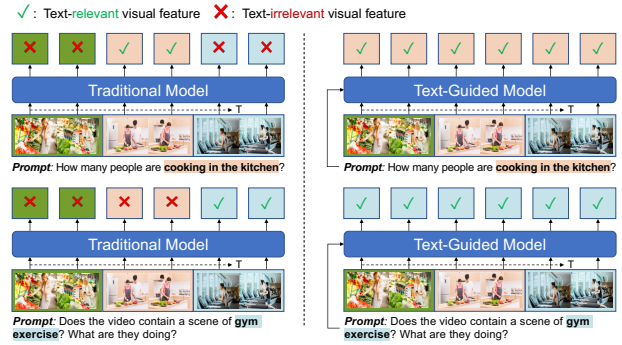

Figure 1. This illustration contrasts traditional and text-guided models. **Left:** The traditional model interprets visual patches directly into tokens for LLMs without considering specific frames or areas of interest. As a result, whether the inquiry belongs to a "kitchen" or a "gym," the model consistently produces the same tokens and applies uniform attention to all details in the scene, potentially increasing the cognitive burden on the LLMs. **Right:** The text-guided model utilizes prompts to identify the most relevant visual cues and generates adaptive tokens, thereby improving the LLMs' capacity to comprehend and interpret visual information.

content that spans several minutes. This task is highly valuable because long-form videos, ranging from educational tutorials to feature films, play a crucial role in our everyday life. When people want to seek specific knowledge in a long video, a quick way is to first identify and locate relevant segments of the video according to the intention. Then, we focus on the content of those segments, paying attention to highly related information rather than treating every frame in the same manner. Whereas most existing video understanding models [7, 32, 42, 45–47] treat all input frames indiscriminatingly, leading to output visual tokens that contain significant redundant information, especially in untrimmed videos containing diverse scenes. These models either scale up or increase the number of visual tokens provided to the LLM. Unfortunately, integrating long visual sequences into Large Language Models (LLMs) raises addi-
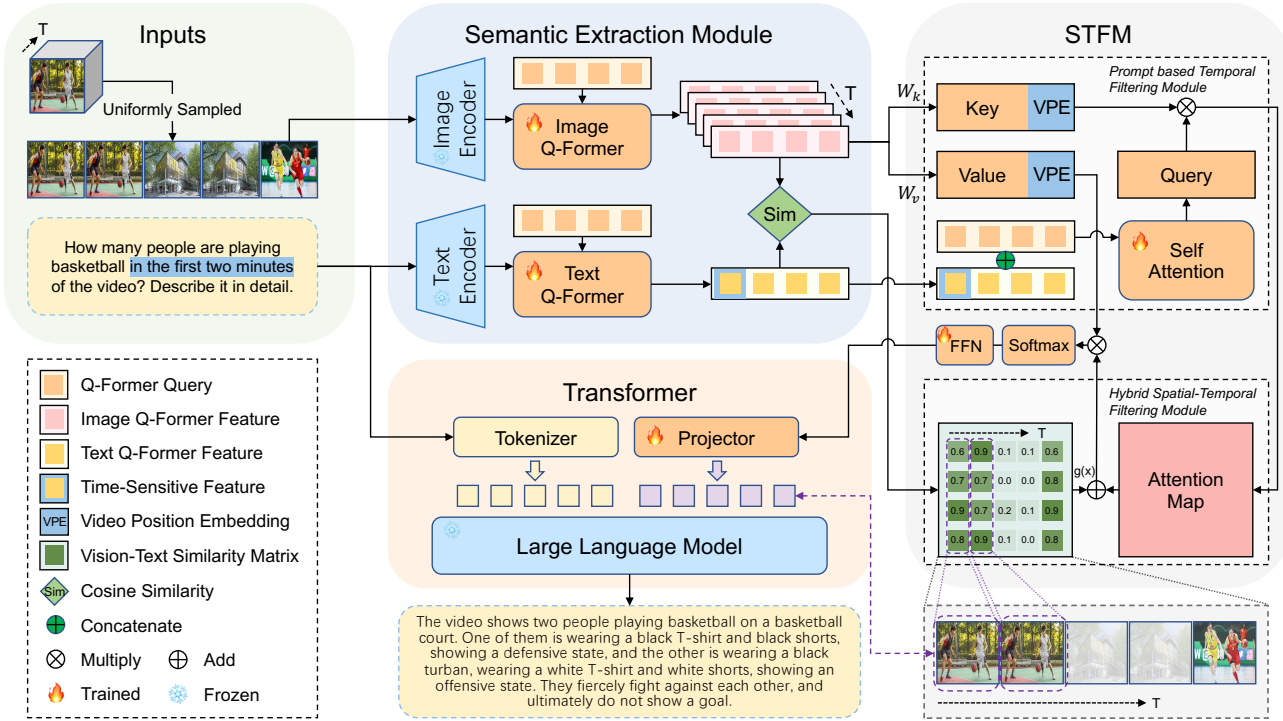
Figure 2. The overall architecture of FocusChat: uniformly sampled frames are input into the vision semantic branch, which consists of an image encoder and an image Q-Former. Simultaneously, the user's query is input into the text semantic branch to extract rich semantic representations. Finally, these are fused in STFM to achieve both spatial-level and temporal-level filtering of visual information. The output of STFM is projected as visual tokens, which are fed into the LLM along with the text tokens.

tional complexities. As shown in Fig. 1 , no matter whether the query is "How many people are cooking in the kitchen?" or "Does the video contain a scene of gym exercise? What are they doing?" The traditional model transforms the video into identical tokens, resulting in redundancy of information. In contrast, the text-guided model extracts visual information based on the query content, enhancing the model's capabilities via concentration.

In order to address the aforementioned issues, we propose a text-guided model for long video understanding. The core idea is to extract visual content that closely aligns with the user's prompt. We leverage the image Q-Former from Video-LLaMA [71] to extract visual and text information. The visual and textual semantic representations are then fed into a Spatial-Temporal Filtering Module (STFM). As shown in Fig. 2, the two submodules of STFM, which are the prompt-based temporal filtering (PBTF) module and the hybrid spatial-temporal filtering (HSTF) module, together make the generated visual tokens closely related to the semantics of the user's query.

The PBTF module extracts visual features consistent with the semantics of the prompt, and the HSTF module adopts a vision-text similarity matrix to filter visual tokens from both spatial and temporal perspectives. As shown in

Fig. 1 , when the user asks: "How many people are playing basketball in the first two minutes?", the model's response has nothing to do with scenes after the first two minutes and scenes not containing playing basketball. PBTF adopts time-sensitive tokens of the words "first two minutes" as queries to filter the keys and values of visual information. Meanwhile, HSTF omits scenes and regions with low correlations with the query via the vision-text similarity matrix. Ultimately, only features corresponding to the query are used as visual tokens. A novel vision position embedding approach is proposed to facilitate the filtering process. **We summarize our contributions as follows:**

- We propose a novel approach called FocusChat with a Spatial-Temporal Filtering Module to align the visual tokens properly with the prompt. Specifically, two submodules of STPM are proposed (Prompt-based temporal filtering module and hybrid spatial-temporal filtering module) to generate efficient and effective visual tokens.

- FocusChat achieves competitive results in zero-shot and few-shot experiments with only an order of magnitude fewer data and even 16 visual tokens occupied, making it much easier to use in practice.

2

- We conducted thorough ablation experiments on each module in STFM. The results demonstrate that the proposed method is both efficient and effective.

2. Related Work

Large Language Models (LLMs). Language is a key skill for expression and communication in humans, which begins to develop in early childhood and continues to evolve throughout life [15, 38]. Enabling machines to read, write, and communicate like humans has long been a challenging research goal [51] that is significant for human development. LLM is currently a popular way to implement such functionality. Typically, large language models (LLMs) refer to transformer language models [52] that contain hundreds of billions (or more) of parameters, which are trained on massive text data [44], such as GPT-3 [34], PaLM [9], Galactica [48], and LLaMA [49]. LLMs exhibit strong capacities to understand natural language and solve complex tasks (via text generation).

Vision Large Language Models (vLLMs). The integration of the perceptual abilities of the vision models [21, 35, 37, 40] with the reasoning capabilities of LLMs has given rise to Vision Large Language Models (vLLMs) [17, 27, 66]. VLLMs encompass both Image-Language and Video-Language models. This approach transforms visual signals into tokens interpretable by LLMs. Image-Language models integrate powerful pre-trained language models with image encoders to enhance multi-modal reasoning capabilities [23, 30, 73]. For instance, Flamingo [1] connects state-of-the-art vision-only and language-only models to excel in few-shot learning tasks. BLIP-2 [23] introduces a lightweight querying transformer to bridge the gap between frozen image encoders and language models, achieving strong performance with fewer trainable parameters. LLaVA [30] utilizes a simple linear layer to project image features into the text embedding space, effectively fine-tuning language models for improved outcomes. MiniGPT-4 builds on BLIP-2 [73] by gathering a large dataset of image-text pairs, enhancing language generation. Video-language models have evolved from image-language models like Flamingo [1] and BLIP-2 [23], which flatten spatio-temporal features into 1D sequences but struggle to capture temporal dynamics. Models such as Video-LLaMA [71] add video querying transformers to enhance temporal understanding, while Video-ChatGPT [33] averages spatial-level features for video representation. ChatVideo [53] uses tracklets annotated with textual descriptions and employs ChatGPT for various tasks, while VideoChat [24] generates action and object annotations for LLM reasoning.

Long Video Understanding. Long video understanding poses significant challenges in computer vision, primarily because it requires capturing long-range patterns in videos that often exceed 30 seconds. A typical strategy [3, 6, 55] involves maintaining a memory bank to store historical information and utilizing parametric [55] or non-parametric [3] compression modules to manage this efficiently. Recent approaches [16, 19, 41] have also integrated language as a bridge for understanding, breaking long videos into shorter clips, generating textual descriptions for each, and then employing large language models (LLMs) to aggregate these captions for analysis. However, these methods are cumbersome and lack conciseness. Some have adopted streaming methods [16, 39, 42, 72] to process long videos. Although these methods appear promising, indiscriminately handling all video frames inevitably leads to information redundancy. [47] is a key-frame-based model, distinct from previous methods. Although it appears to treat each frame differently, the key frame is fixed and unrelated to the prompt. Our proposed text-guided approach effectively addresses this issue. There are very few video understanding models based on this method, with [39] being one of them. However, it has several drawbacks, including a complex model structure, time-consuming computations, and an inability to filter information at the frame level or even at the region level. In contrast, our FocusChat effectively overcomes these limitations.

3. Method

We present FocusChat, which consists of the semantic extraction module and STFM. The former includes the vision branch and the text branch, which will be introduced in Sec. 3.1. These branches are subsequently merged in STFM, which will be discussed in Sec. 3.2.

3.1. Semantic Extraction Module

The semantic extraction module includes vision and text semantic branches. It extracts user prompt and visual features. These semantic features are then fed into STFM, which filters the image semantics using the text semantics to get visual features closely related to intention.

3.1.1 Visual Semantic Branch

The visual semantic branch extracts the semantic information from each image. It consists of a frozen pre-trained image encoder and an image Q-Former. A video consists of T frames is represented as $\mathbf{V} \in \mathbb{R}^{T \times H \times W \times 3}$. The input frames are passed into a pre-trained visual encoder, i.e., ViT, to obtain the visual frame features $\mathbf{V_f} \in \mathbb{R}^{T \times N_v \times C}$, where N_v represents the number of patches, and C denotes the number of feature channels. Subsequently, an image Q-Former further compresses the frame features. As Fig. 2 illustrates, the image Q-Former takes as input M learnable queries of length D. These queries interact with the frame features via cross-attention and update the initial queries to
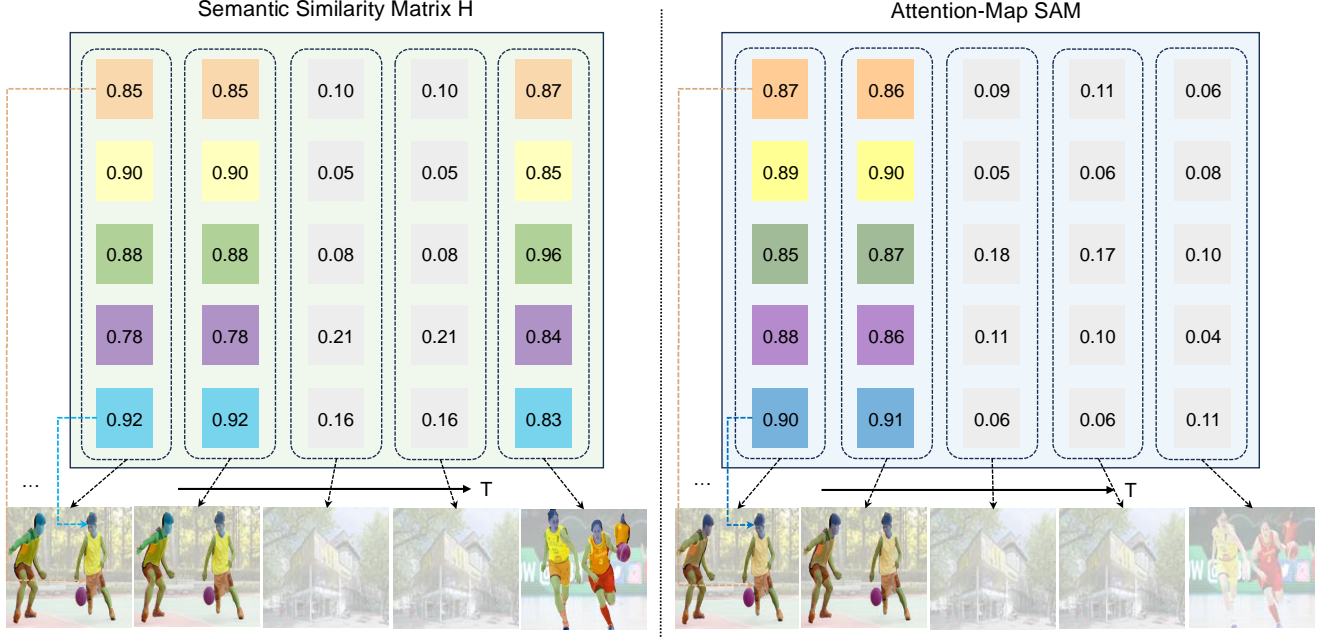
Figure 3. When asking a question about a five-minute video, such as "How many people are playing basketball in the first two minutes? Describe it in detail," the semantic similarity matrix H and the attention-map SAM diagram in STFM are presented.

output the final *M* visual semantic vectors of length *D*, denoted as $\mathbf{V_q} \in \mathbb{R}^{T \times M \times D}$. Each visual vector contains semantic information at the region level or frame level. For example, the visual semantics extracted from the video in Fig. 1 may include elements such as men, women, vegetables, treadmills, etc.

3.1.2 Textual Semantic Branch

The text semantic branch is designed to semantically encode the user's input prompt *P*. A pre-trained CLIP [40] model encodes the user prompt, resulting in prompt features $\mathbf{P_f} \in \mathbb{R}^{N_p \times D}$, where *D* denotes the dimension of text embedding, and N_p is the text token number. We then employ a Q-Former, similar to the visual semantic branch, to encode $\mathbf{P_f}$. In this process, $\mathbf{P_f}$ is projected as keys and values. By utilizing *M* trainable query embeddings, we obtain *M* text vectors, denoted as $\mathbf{P_q} \in \mathbb{R}^{M \times D}$. Each textual vector contains semantic information at the word or sub-word level. For example, the prompt "How many people are cooking in the kitchen?" in Fig. 1 may be parsed into semantic vectors such as person, cooking, kitchen, etc.

3.2. Spatial-Temporal Filtering Module (STFM)

3.2.1 Hybrid Spatial-Temporal Filtering Module

To obtain visual features that are semantically close to the user's query, we first compute the semantic similarity matrix by calculating the similarity between text and visual se-

mantic vectors. The similarity matrix is then used to guide the hybrid spatial-temporal filtering (HSTF) module for visual information filtering. The filtering process is explicitly applied to the video in both spatial and temporal dimensions. Spatial filtering is performed row by row, as shown in Fig. 2, while temporal filtering is applied column by column.

Semantic Similarity Matrix. We compute the cosine similarity between the text semantic feature $\mathbf{P_q}$ and the visual semantic feature $\mathbf{V_q}$ to get the similarity matrix $\mathbf{H} \in \mathbb{R}^{T \times M}$. As shown in Eq. (1), *sim* indicates cosine similarity and normalization, *t* is the frame index, and *i* is the semantic feature index. Since text semantics can achieve word-level granularity and visual semantics can achieve region-level granularity, therefore $\mathbf{H}$ represents fine-grained similarity. For example, in Fig. 3, each element of the semantic similarity matrix H represents a specific region in the image, such as an arm, body, or basketball. It serves as a guide for filtering the visual spatial-temporal features.

$$ H_{t,i} = sim(V_{q_{t,i}}, P_{q_i}) = \left(\frac{V_{q_{t,i}} \cdot P_{q_i}}{\| V_{q_{t,i}} \| \times \| P_{q_i} \|} + 1 \right) \times \frac{1}{2} \quad (1) $$

The Video Q-Former in Video-LLaMA [71] treats all frames indiscriminately. We improved the Video Q-Former by enabling it to receive a semantic similarity matrix to filter visual features based on its values. This process occurs in cross-attention of STFM, allowing FocusChat to extract accurate vision semantics related to the user's question more

effectively and explicitly. As a result, it enhances the accuracy and generalization ability of FocusChat while reducing the load on the LLM.

Hybrid Spatial-Temporal Filtering Cross-Attention. The input to STFM consists of trainable queries, which are fed into self-attention, resulting in $\mathbf{V_s} \in \mathbb{R}^{N \times d}$, where N is the number of queries. Given $\mathbf{V_s}$, semantic similarity matrix $\mathbf{H}$, and the visual semantic feature $\mathbf{V_q}$, as shown in Fig. 2, we aim to produce an attention map that is closely related to the semantic similarity matrix. We first project $\mathbf{V_q}$ to generate keys and values using $\mathbf{W_k}$ and $\mathbf{W_v}$. Our hybrid spatial-temporal filtering module based attention-map $\mathbf{SAM} \in \mathbb{R}^{N \times TM}$ is given in Eq. (2), which is equivalent to $SAM = softmax(\alpha log H + QK^T/\sqrt{d})$, where α is a constant greater than or equal to 0. So $g(x) = \alpha log x$ as shown in Fig. 2. The output of the hybrid spatial-temporal filtering module is denoted as $\mathbf{Z} \in \mathbb{R}^{N \times d}$. Eq. (2) and Eq. (3) complete most of the spatiotemporal information filtering. Therefore, the redundant information filtered in $\mathbf{V_q}$ alleviates the pressure on the number of vision tokens sent to LLM.

$$SAM_{j,i} = \frac{H_i^{\alpha} e^{V_{s_i} W_q (V_{q_i} W_k)^T / \sqrt{d}}}{\sum_{i=1}^{TM} H_i^{\alpha} e^{V_{s_i} W_q (V_{q_i} W_k)^T / \sqrt{d}}} \quad (2)$$

$$Z_j = LayerNorm(\sum_{i=1}^{TM} H_i^{\beta} SAM_{j,i} V_{q_i} W_v) \quad (3)$$

Through the HSTF process, we obtain visual-semantic features highly relevant to the user's prompt. As shown in Fig. 3, useful semantic information from all frames is extracted, while irrelevant visual-semantic features are filtered out.

3.2.2 Prompt Based Temporal Filtering Module

The visual features highly relevant to the question are extracted with the help of HSTF. However, there are still some redundant temporal information unfiltered. For example, in the left image of Fig. 3, the semantic information from the last minute is encoded into the visual tokens. For these time-sensitive questions, we use prompt based temporal filtering(PBTF) module to better extract the features in temporal dimension. We first add a temporal position encoding to $\mathbf{V_q}$. Unlike the trainable position encoding used in the original Video-LLaMA, we design a position encoding based on the transformer's [52] model. Experiments indicate that the revised position encoding is more effective. Furthermore, it facilitates the development of a multi-modal model with extrapolation capabilities in the future. The traditional transformer's [52] position embedding is shown in Eq. (4), where *pos* represents the position, specifically the frame index here. *i* denotes the dimension, and *d* is the feature dimension. We improve upon it by substituting **VPE** for *pos*,

Modality	dataset	Original	Used	Ratio
Video-Text	webvid [2]	10M	0.62M	6.2%
Image-Text	CC-3M [4]	3M	0.10M	3%
total	-	13M	0.72 M	5.5%

Table 1. Zero-shot pre-training data details.

Hyper-parameter	first stage	second stage
α in **STFM**	1	
β in **STFM**	0	
S in **VPE**	500	
Number of video tokens	32	
Number of all Q-Former queries	32	
Number of input frames T	15	
Max text length	2048	
Epochs	1	
Batch size	128	
Weight decay	0.05	
AdamW β	(0.9, 0.999)	
Warm-up learning rate	1e-6	
LLM	LLaMA2-7B	
Learning rate	1e-4	3e-5

Table 2. Hyper-parameters of two training stages.

where $VPE = pos \cdot (S/T)$, and S is a constant. The ablation experiments demonstrate that our VPE enhances the effectiveness of STFM.

$$PE_{(pos,2i)} = sin(pos/10000^{2i/d})$$
$$PE_{(pos,2i+1)} = cos(pos/10000^{2i/d}) \quad (4)$$

3.3. Model Training

3.3.1 Zero-Shot Training

To train FocusChat, we design a two-stage paradigm. We use a total of 1.5 million data samples for zero-shot training. **In the first stage**, The pre-training data is detailed in Tab. 1. We utilize part of the picture description pairs from CC-3M [4] and video description pairs from WebVid [2], totaling approximately only 0.72 million pairs. Since there are no user instructions at this stage, we construct various instruction templates, such as "Describe this video in detail," and randomly select templates to generate user input during training. The components that can be optimized in this stage include the image Q-Former, text Q-Former, projector, and STFM. **In the second stage**, we retain the trainable modules from the previous stage but use different training data VideoChat2-IT [25], which includes NExTQA [58], TextVR [57], CLEVRER [68], TGIF [28], Kinetics-710 [20], EgoQA [12], ShareGPT4Video [5], etc. We sam-

ple a small subset of data from VideoChat2-IT as the fine-tuning dataset, totaling approximately 0.8M, reformulating their instructions to fit the specific structure of FocusChat.

3.3.2 Few-Shot Training

To more comprehensively evaluate the model's performance, we conducted few-shot training in addition to zero-shot experiments. The few-shot training is based on the zero-shot model. We use the semantic extraction module of the zero-shot fine-tuned model and the remaining modules of the pre-trained model as the initialization for few-shot training. The parameters of the semantic extraction module are fixed, and only the STFM module and the projection layer are optimized to ensure consistency and stability in semantic extraction. In this phase, we train on each benchmark separately, with the data details provided in Sec. 4.2.

4. Experiments

4.1. Implementation Details

We use the ViT-G/14 from EVA-CLIP [13] as the image encoder and CLIP [40] as the text encoder to ensure that the extracted text features and corresponding visual features are aligned in the embedding space. The image Q-Former and text Q-Former are initialized with the InstructBLIP's [11] checkpoint, while the text Q-Former and video Q-Former are randomly initialized. We use the open-source LLaMA2 (7B) model as the LLM. In STFM, the parameters α and β are set to 1 and 0, respectively, and the number of queries for all Q-Formers is 32. Hyper-parameters for all three zero-shot training stages are provided in Tab. 2. The few-shot training parameters are the same as those for zero-shot, except for the learning rate, which is set to 5e-5. Each few-shot training sample also includes the instruction: "Please answer as briefly as possible."

4.2. Datasets

Our zero-shot model evaluation benchmarks include ActivityNet-QA [70], MSVD-QA [60], MSRTT-QA [60], and MovieChat1K [45], all of which are open-ended visual question-answering datasets. Except for MovieChat1K [45] with an average duration of 8 minutes, the video durations of the other datasets are around 1 to 2 minutes. For these evaluations, we use the widely adopted GPT-3.5-Turbo. For the few-shot experiments, we conduct training and testing on ActivityNet-QA [70], MSVD-QA [60], MSRTT-QA, and Next-QA [60]. Next-QA [58] has an average duration of 42 seconds and is a multiple-choice dataset. Since there is no standardized evaluation method for open-domain visual question-answering datasets in few-shot tasks, we used two evaluation approaches for all datasets except Next-QA [58]: one with GPT-3.5-Turbo and another with a strict evaluation method, where a prediction is considered correct only if it exactly matches the ground truth.

4.3. Main Results

Zero-Shot Result. For the quantitative experiments, we use a very small training dataset of approximately 1.5 million samples, which makes a direct comparison with models trained on tens of millions of unfair to some extent. Our model is an improvement on the Video-LLaMA structure. Thus, we mainly compared FocusChat with Video-LLaMA. Video-LLaMA uses a dataset of tens of millions of samples, whereas we use only about one-tenth of that amount. Despite this, FocusChat outperforms Video-LLaMA across all benchmarks.

As shown in Tab. 4, on the ActivityNet-QA dataset, FocusChat's accuracy exceeds Video-LLaMA by 20.8, with a score improvement of around 2. On the MSRTT-QA dataset, FocusChat's accuracy surpasses Video-LLaMA by 17, with a score increase of 1.4. For MovieChat1K, we only test the global model, and FocusChat's accuracy outperforms Video-LLaMA by 8.3, demonstrating FocusChat's superior ability to understand long videos. On the MSVD-QA dataset, FocusChat matches Video-LLaMA in accuracy, with its score 0.94 higher.

FocusChat's average score across all datasets is approximately 3.3, reflecting the high quality of its responses. FocusChat uses a smaller dataset compared with some other "SOTA" models, with model complexity nearly identical to that of Video-LLaMA. For the qualitative experiments, we compared the zero-shot performance of Video-LLaMA and FocusChat, as shown in Fig. 4, which demonstrates the accuracy of our model's responses to different types of user prompts.

Few-Shot Result. To further validate the effectiveness of FocusChat, we conduct few-shot experiments based on a zero-shot model on open-domain visual question-answering datasets ActivityNet-QA, MSVD-QA, MSRTT-QA, and the multiple-choice dataset Next-QA. As shown in Tab. 3, we compare recent few-shot models on these datasets, many of which use quite large pre-training datasets. For instance, VideoCoCa achieves state-of-the-art performance on ActivityNet-QA with a pre-training dataset size as large as 4.8B, whereas our model only uses 0.72M pre-training data, still yields comparable results with SOTA performance. FocusChat gets 63.7 with GPT-3.5-Turbo evaluation on MSVD-QA, 54.6 without GPT-3.5-Turbo evaluation. The accuracy on Next-QA is 68.20, second only to the SeViLA model. This demonstrates the significant potential of FocusChat.

4.4. Ablation Study

To verify the effectiveness and rationality of FocusChat's design, we conduct few-shot and zero-shot ablation experi-

method	PT	Activitynet-QA	MSVD-QA	MSRTT-QA	Next-QA
JustAsk [64]	69M	38.9	47.5	41.8	50.8
FrozenBiLM [65]	400M	43.2	54.8	47.0	-
Singularity [22]	17M	44.1	-	43.5	-
VIOLETv2 [14]	5M	44.5	54.7	-	-
GiT [54]	800M	43.2	56.8	-	-
mPLUG-2 [61]	17M	48.0	58.1	-	-
UMT-L [26]	25M	47.9	55.2	47.1	-
VideoCoCa [63]	4.8B	**56.1**	56.9	46.3	-
MA-LMM [16]	-	<u>49.8</u>	<u>60.6</u>	<u>48.5</u>	-
SeViLA [69]	129M	-	-	-	**73.4**
HiTeA [67]	5M	45.1	55.6	45.4	63.1
IGV [29]	-	-	40.8	38.3	51.3
HQGA [59]	-	-	41.2	38.6	51.8
FocusChat	0.72M	42.5	54.6	45.4	<u>68.20</u>
FocusChat*	0.72M	49.4*	**63.7***	**54.4***	-

Table 3. The few-shot evaluation results of various models on ActivityNet-QA, MSVD-QA, MSRTT-QA, and Next-QA. * indicates GPT-3.5-Turbo evaluation, while no * means non-GPT-3.5-Turbo evaluation. Bold represents the first place, and the underscore indicates the second place. PT refers to the number of pre-training datasets.

benchmark method	Activitynet-QA acc/score	MSVD-QA acc/score	MSRTT-QA acc/score	Moviechat1k acc/score
Video-LLaMA	12.4/1.1	51.6/2.5	29.6/1.8	51.7/2.57
FocusChat	33.2/3.1	52.4/3.4	46.7/3.2	60.0/3.54
difference value	+20.8/+2.0	+0.8/+0.9	+17.1/+1.4	+8.3/+0.97

Table 4. The zero-shot evaluation results of FocusChat and Video-LLaMA on the ActivityNet-QA, MSVD-QA, MSRTT-QA, and MovieChat1K datasets, with the "difference value" representing the performance gap where FocusChat exceeds Video-LLaMA.

method	Accuracy
Video-LLaMA	45.07
baseline(Video-LLaMA w/ **VPE**+ln)	47.34
ours(baseline+α=0+β=1)	48.17
ours(baseline+α=0.5+β=1)	48.55
ours(baseline+α=1+β=1)	48.85
ours(baseline+α=1+β=0)	48.93
ours(baseline+α=1+β=1+PBTF)	49.05
FocusChat(baseline+α=1+β=0+PBTF)	**49.40**
FocusChat wo **VPE**	49.29

Table 5. Ablation of the few-shot results for each module parameter of FocusChat on ActivityNet-QA benchmark.

method	PT/FT	NT	Acc/score
Video-LLaMA	Millions/Millions	32	12.4/1.1
FocusChat	0.72M/0.8M	32	33.2/3.1
FocusChat(16)	0.72M/0.8M	16	27.7/2.8

Table 6. Ablation of the zero-shot results for the number of vision tokens on ActivityNet-QA benchmark. PT represents the amount of pretraining data, FT represents the amount of fine-tuning data, and NT represents the number of vision tokens to LLM.

ments based on the ActivityNet-QA dataset.

For few-shot ablation, each experiment in Tab. 5 involves pre-training and fine-tuning, with the same data used as in the previous zero-shot experiments. Since our model architecture is similar to Video-LLaMA, we use it as a reference for comparison. The "baseline" in Tab. 5 refers to replacing the trainable positional encoding in Video-LLaMA's video Q-Former with our proposed absolute positional encoding **VPE** and adding an LN layer to each layer of the video Q-Former, as shown in Eq. (3). This improvement increased the model accuracy from 45.07 to 47.34. Rows from 2 to 6 in Tab. 5 show the impact of different alpha and beta parameter values in the STFM module on model performance. The optimal parameters were $\alpha = 1$ and $\beta = 0$, resulting in an accuracy of 48.93, an improvement of 1.59 over the baseline. This demonstrates that the effec-
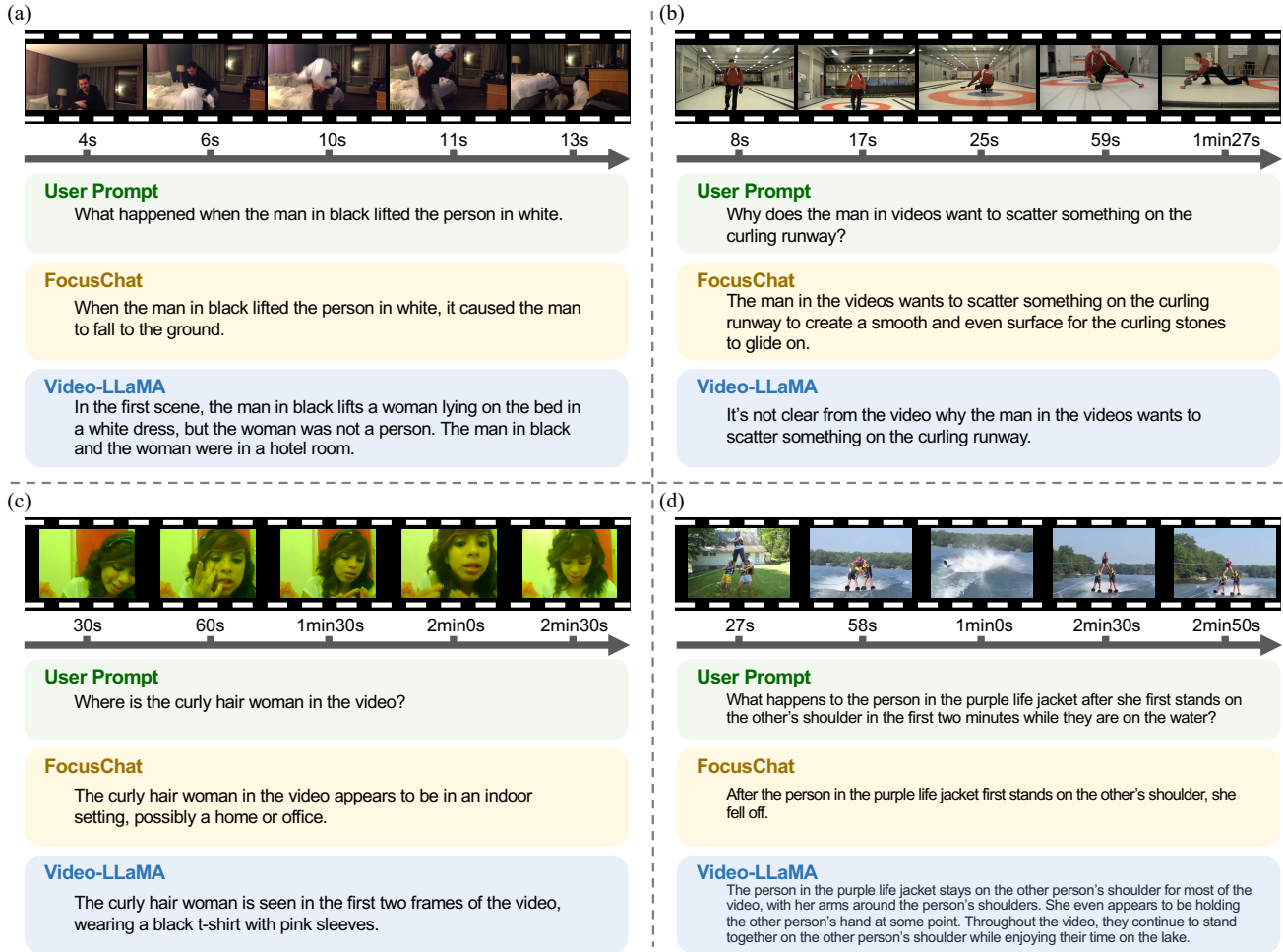
Figure 4. Qualitative result comparison between Video-LLaMA and FocusChat.

tiveness of the spatial-level feature filtering process aligning with prompt semantics. Rows of 7 and 8 in Tab. 5 introduce ablation of prompt-based temporal filtering (PBTF) module. With this addition, FocusChat's accuracy increased to 49.4, validating the effectiveness of time-level feature filtering. Finally, to further confirm the effectiveness of **VPE**, we replaced the positional encoding in FocusChat with the original trainable positional encoding from Video-LLaMA. The accuracy dropped to 49.29, reaffirming the validity of the proposed positional encoding block.

The zero-shot ablation experiment was conducted to verify the impact to the number of vision tokens on model performance. This experiment was also performed on ActivityNet-QA. We train a FocusChat model with 16 vision tokens, denoted as FocusChat (16). As shown in Tab. 6, even with 16 vision tokens, 0.72M pretraining data, and 0.8M fine-tuning data, the model accuracy surpassed Video-LLaMA by 15.3, with only 5.5 points drop compared to FocusChat. This demonstrates that the effectiveness of

our model in extracting visual features lowers the essential acount of vision tokens needed.

5. Conclusion

In this paper, we introduce FocusChat, a text-guided model that employs spatiotemporal information filtering to realize the efficiency of visual information. As far as we know, we are the first to explore redundant spatiotemporal information filtering of visual features. The extracted visual tokens properly aligning with the user's input elevate the model's vision understanding capacity. Experiments confirm the effectiveness of FocusChat. In few-shot experiments, it obtained competitive performance on par with SOTA models, with only 10 percent of the pre-training data. It outperforms Video-LLaMA in zero-shot tasks with only 16 visual tokens used and a magnitude less data. Besides the research value, the proposed method will show its advantages in practical and constrained scenarios.

References

[1] Jean-Baptiste Alayrac, Jeff Donahue, Pauline Luc, Antoine Miech, Iain Barr, Yana Hasson, Karel Lenc, Arthur Mensch, Katherine Millican, Malcolm Reynolds, et al. Flamingo: a visual language model for few-shot learning. *Advances in neural information processing systems*, 35:23716–23736, 2022. 3

[2] Max Bain, Arsha Nagrani, Gül Varol, and Andrew Zisserman. Frozen in time: A joint video and image encoder for end-to-end retrieval. In *Proceedings of the IEEE/CVF international conference on computer vision*, pages 1728–1738, 2021. 5

[3] Ivana Balažević, Yuge Shi, Pinelopi Papalampidi, Rahma Chaabouni, Skanda Koppula, and Olivier J Hénaff. Memory consolidation enables long-context video understanding. *arXiv preprint arXiv:2402.05861*, 2024. 3

[4] Soravit Changpinyo, Piyush Sharma, Nan Ding, and Radu Soricut. Conceptual 12m: Pushing web-scale image-text pre-training to recognize long-tail visual concepts. In *Proceedings of the IEEE/CVF conference on computer vision and pattern recognition*, pages 3558–3568, 2021. 5

[5] Lin Chen, Xilin Wei, Jinsong Li, Xiaoyi Dong, Pan Zhang, Yuhang Zang, Zehui Chen, Haodong Duan, Bin Lin, Zhenyu Tang, et al. Sharegpt4video: Improving video understanding and generation with better captions. *arXiv preprint arXiv:2406.04325*, 2024. 5

[6] Ho Kei Cheng and Alexander G Schwing. Xmem: Long-term video object segmentation with an atkinson-shiffrin memory model. In *European Conference on Computer Vision*, pages 640–658. Springer, 2022. 3

[7] Zesen Cheng, Sicong Leng, Hang Zhang, Yifei Xin, Xin Li, Guanzheng Chen, Yongxin Zhu, Wenqi Zhang, Ziyang Luo, Deli Zhao, et al. Videollama2: Advancing spatial-temporal modeling and audio understanding in video-llms. *arXiv preprint arXiv:2406.07476*, 2024. 1

[8] Wei-Lin Chiang, Zhuohan Li, Zi Lin, Ying Sheng, Zhanghao Wu, Hao Zhang, Lianmin Zheng, Siyuan Zhuang, Yonghao Zhuang, Joseph E Gonzalez, et al. Vicuna: An open-source chatbot impressing gpt-4 with 90%* chatgpt quality. *See https://vicuna. lmsys. org (accessed 14 April 2023)*, 2(3):6, 2023. 1

[9] Aakanksha Chowdhery, Sharan Narang, Jacob Devlin, Maarten Bosma, Gaurav Mishra, Adam Roberts, Paul Barham, Hyung Won Chung, Charles Sutton, Sebastian Gehrmann, et al. Palm: Scaling language modeling with pathways. arxiv 2022. *arXiv preprint arXiv:2204.02311*, 10, 2022. 3

[10] Hyung Won Chung, Le Hou, Shayne Longpre, Barret Zoph, Yi Tay, William Fedus, Yunxuan Li, Xuezhi Wang, Mostafa Dehghani, Siddhartha Brahma, et al. Scaling instruction-finetuned language models. *Journal of Machine Learning Research*, 25(70):1–53, 2024. 1

[11] Wenliang Dai, Junnan Li, Dongxu Li, Anthony Meng Huat Tiong, Junqi Zhao, Weisheng Wang, Boyang Li, Pascale Fung, and Steven Hoi. Instructblip: Towards general-purpose vision-language models with instruction tuning. 2023. 6

[12] Chenyou Fan. Egovqa-an egocentric video question answering benchmark dataset. In *Proceedings of the IEEE/CVF International Conference on Computer Vision Workshops*, pages 0–0, 2019. 5

[13] Yuxin Fang, Wen Wang, Binhui Xie, Quan Sun, Ledell Wu, Xinggang Wang, Tiejun Huang, Xinlong Wang, and Yue Cao. Eva: Exploring the limits of masked visual representation learning at scale. In *Proceedings of the IEEE/CVF Conference on Computer Vision and Pattern Recognition*, pages 19358–19369, 2023. 6

[14] Tsu-Jui Fu, Linjie Li, Zhe Gan, Kevin Lin, William Yang Wang, Lijuan Wang, and Zicheng Liu. An empirical study of end-to-end video-language transformers with masked visual modeling. In *Proceedings of the IEEE/CVF Conference on Computer Vision and Pattern Recognition*, pages 22898–22909, 2023. 7

[15] Marc D Hauser, Noam Chomsky, and W Tecumseh Fitch. The faculty of language: what is it, who has it, and how did it evolve? *science*, 298(5598):1569–1579, 2002. 3

[16] Bo He, Hengduo Li, Young Kyun Jang, Menglin Jia, Xuefei Cao, Ashish Shah, Abhinav Shrivastava, and Ser-Nam Lim. Ma-lmm: Memory-augmented large multimodal model for long-term video understanding. In *Proceedings of the IEEE/CVF Conference on Computer Vision and Pattern Recognition*, pages 13504–13514, 2024. 3, 7

[17] Shengding Hu, Yuge Tu, Xu Han, Chaoqun He, Ganqu Cui, Xiang Long, Zhi Zheng, Yewei Fang, Yuxiang Huang, Weilin Zhao, et al. Minicpm: Unveiling the potential of small language models with scalable training strategies. *arXiv preprint arXiv:2404.06395*, 2024. 3

[18] Peng Jin, Ryuichi Takanobu, Wancai Zhang, Xiaochun Cao, and Li Yuan. Chat-univi: Unified visual representation empowers large language models with image and video understanding. In *Proceedings of the IEEE/CVF Conference on Computer Vision and Pattern Recognition*, pages 13700–13710, 2024. 1

[19] Kumara Kahatapitiya, Kanchana Ranasinghe, Jongwoo Park, and Michael S Ryoo. Language repository for long video understanding. *arXiv preprint arXiv:2403.14622*, 2024. 3

[20] Will Kay, Joao Carreira, Karen Simonyan, Brian Zhang, Chloe Hillier, Sudheendra Vijayanarasimhan, Fabio Viola, Tim Green, Trevor Back, Paul Natsev, et al. The kinetics human action video dataset. *arXiv preprint arXiv:1705.06950*, 2017. 5

[21] Alexander Kirillov, Eric Mintun, Nikhila Ravi, Hanzi Mao, Chloe Rolland, Laura Gustafson, Tete Xiao, Spencer Whitehead, Alexander C Berg, Wan-Yen Lo, et al. Segment anything. In *Proceedings of the IEEE/CVF International Conference on Computer Vision*, pages 4015–4026, 2023. 3

[22] Jie Lei, Tamara L Berg, and Mohit Bansal. Revealing single frame bias for video-and-language learning. *arXiv preprint arXiv:2206.03428*, 2022. 7

[23] Junnan Li, Dongxu Li, Silvio Savarese, and Steven Hoi. Blip-2: Bootstrapping language-image pre-training with frozen image encoders and large language models. In *International conference on machine learning*, pages 19730–19742. PMLR, 2023. 3

[24] KunChang Li, Yinan He, Yi Wang, Yizhuo Li, Wenhai Wang, Ping Luo, Yali Wang, Limin Wang, and Yu Qiao. Videochat: Chat-centric video understanding. *arXiv preprint arXiv:2305.06355*, 2023. 1, 3

[25] Kunchang Li, Yali Wang, Yinan He, Yizhuo Li, Yi Wang, Yi Liu, Zun Wang, Jilan Xu, Guo Chen, Ping Luo, et al. Mvbench: A comprehensive multi-modal video understanding benchmark. In *Proceedings of the IEEE/CVF Conference on Computer Vision and Pattern Recognition*, pages 22195–22206, 2024. 5

[26] Kunchang Li, Yali Wang, Yizhuo Li, Yi Wang, Yinan He, Limin Wang, and Yu Qiao. Unmasked teacher: Towards training-efficient video foundation models. In *Proceedings of the IEEE/CVF International Conference on Computer Vision*, pages 19948–19960, 2023. 7

[27] Xiaotong Li, Fan Zhang, Haiwen Diao, Yueze Wang, Xinlong Wang, and Ling-Yu Duan. Densefusion-1m: Merging vision experts for comprehensive multimodal perception. *arXiv preprint arXiv:2407.08303*, 2024. 3

[28] Yuncheng Li, Yale Song, Liangliang Cao, Joel Tetreault, Larry Goldberg, Alejandro Jaimes, and Jiebo Luo. Tgif: A new dataset and benchmark on animated gif description. In *Proceedings of the IEEE Conference on Computer Vision and Pattern Recognition*, pages 4641–4650, 2016. 5

[29] Yicong Li, Xiang Wang, Junbin Xiao, Wei Ji, and Tat-Seng Chua. Invariant grounding for video question answering. In *Proceedings of the IEEE/CVF Conference on Computer Vision and Pattern Recognition*, pages 2928–2937, 2022. 7

[30] Haotian Liu, Chunyuan Li, Qingyang Wu, and Yong Jae Lee. Visual instruction tuning. *Advances in neural information processing systems*, 36, 2024. 3

[31] Tianrui Liu, Qi Cai, Changxin Xu, Zhanxin Zhou, Jize Xiong, Yuxin Qiao, and Tsungwei Yang. Image captioning in news report scenario. *arXiv preprint arXiv:2403.16209*, 2024. 1

[32] Muhammad Maaz, Hanoona Rasheed, Salman Khan, and Fahad Shahbaz Khan. Video-chatgpt: Towards detailed video understanding via large vision and language models. *arXiv preprint arXiv:2306.05424*, 2023. 1

[33] Muhammad Maaz, Hanoona Rasheed, Salman Khan, and Fahad Shahbaz Khan. Video-chatgpt: Towards detailed video understanding via large vision and language models. *arXiv preprint arXiv:2306.05424*, 2023. 3

[34] Ben Mann, N Ryder, M Subbiah, J Kaplan, P Dhariwal, A Neelakantan, P Shyam, G Sastry, A Askell, S Agarwal, et al. Language models are few-shot learners. *arXiv preprint arXiv:2005.14165*, 1, 2020. 3

[35] Ron Mokady, Amir Hertz, and Amit H Bermano. Clipcap: Clip prefix for image captioning. *arXiv preprint arXiv:2111.09734*, 2021. 1, 3

[36] OpenAI. Introducing chatgpt. 2022. 1

[37] Maxime Oquab, Timothée Darcet, Théo Moutakanni, Huy Vo, Marc Szafraniec, Vasil Khalidov, Pierre Fernandez, Daniel Haziza, Francisco Massa, Alaaeldin El-Nouby, et al. Dinov2: Learning robust visual features without supervision. *arXiv preprint arXiv:2304.07193*, 2023. 3

[38] Steven Pinker. *The language instinct: How the mind creates language*. Penguin uK, 2003. 3

[39] Rui Qian, Xiaoyi Dong, Pan Zhang, Yuhang Zang, Shuangrui Ding, Dahua Lin, and Jiaqi Wang. Streaming long video understanding with large language models. *arXiv preprint arXiv:2405.16009*, 2024. 3

[40] Alec Radford, Jong Wook Kim, Chris Hallacy, Aditya Ramesh, Gabriel Goh, Sandhini Agarwal, Girish Sastry, Amanda Askell, Pamela Mishkin, Jack Clark, et al. Learning transferable visual models from natural language supervision. In *International conference on machine learning*, pages 8748–8763. PMLR, 2021. 3, 4, 6

[41] Kanchana Ranasinghe, Xiang Li, Kumara Kahatapitiya, and Michael S Ryoo. Understanding long videos in one multimodal language model pass. *arXiv preprint arXiv:2403.16998*, 2024. 3

[42] Shuhuai Ren, Linli Yao, Shicheng Li, Xu Sun, and Lu Hou. Timechat: A time-sensitive multimodal large language model for long video understanding. In *Proceedings of the IEEE/CVF Conference on Computer Vision and Pattern Recognition*, pages 14313–14323, 2024. 1, 3

[43] Noam Rotstein, David Bensaïd, Shaked Brody, Roy Ganz, and Ron Kimmel. Fusecap: Leveraging large language models for enriched fused image captions. In *Proceedings of the IEEE/CVF Winter Conference on Applications of Computer Vision*, pages 5689–5700, 2024. 1

[44] Murray Shanahan. Talking about large language models. *Communications of the ACM*, 67(2):68–79, 2024. 3

[45] Enxin Song, Wenhao Chai, Guanhong Wang, Yucheng Zhang, Haoyang Zhou, Feiyang Wu, Haozhe Chi, Xun Guo, Tian Ye, Yanting Zhang, et al. Moviechat: From dense token to sparse memory for long video understanding. In *Proceedings of the IEEE/CVF Conference on Computer Vision and Pattern Recognition*, pages 18221–18232, 2024. 1, 6

[46] Zhende Song, Chenchen Wang, Jiamu Sheng, Chi Zhang, Gang Yu, Jiayuan Fan, and Tao Chen. Moviellm: Enhancing long video understanding with ai-generated movies. *arXiv preprint arXiv:2403.01422*, 2024. 1

[47] Reuben Tan, Ximeng Sun, Ping Hu, Jui-hsien Wang, Hanieh Deilamsalehy, Bryan A Plummer, Bryan Russell, and Kate Saenko. Koala: Key frame-conditioned long video-llm. In *Proceedings of the IEEE/CVF Conference on Computer Vision and Pattern Recognition*, pages 13581–13591, 2024. 1, 3

[48] Ross Taylor, Marcin Kardas, Guillem Cucurull, Thomas Scialom, Anthony Hartshorn, Elvis Saravia, Andrew Poulton, Viktor Kerkez, and Robert Stojnic. Galactica: A large language model for science. *arXiv preprint arXiv:2211.09085*, 2022. 3

[49] Hugo Touvron, Thibaut Lavril, Gautier Izacard, Xavier Martinet, Marie-Anne Lachaux, Timothée Lacroix, Baptiste Rozière, Naman Goyal, Eric Hambro, Faisal Azhar, et al. Llama: Open and efficient foundation language models. *arXiv preprint arXiv:2302.13971*, 2023. 1, 3

[50] Hugo Touvron, Louis Martin, Kevin Stone, Peter Albert, Amjad Almahairi, Yasmine Babaei, Nikolay Bashlykov, Soumya Batra, Prajjwal Bhargava, Shruti Bhosale, et al. Llama2: Open foundation and fine-tuned chat models. *arXiv preprint arXiv:2307.09288*, 2023. 1

[51] A Turing. Computing machinery and intelligence. mind. vol. lix,?. 236. 1950. 3

[52] A Vaswani. Attention is all you need. *Advances in Neural Information Processing Systems*, 2017. 3, 5

[53] Junke Wang, Dongdong Chen, Chong Luo, Xiyang Dai, Lu Yuan, Zuxuan Wu, and Yu-Gang Jiang. Chatvideo: A tracklet-centric multimodal and versatile video understanding system. *arXiv preprint arXiv:2304.14407*, 2023. 3

[54] Jianfeng Wang, Zhengyuan Yang, Xiaowei Hu, Linjie Li, Kevin Lin, Zhe Gan, Zicheng Liu, Ce Liu, and Lijuan Wang. Git: A generative image-to-text transformer for vision and language. *arXiv preprint arXiv:2205.14100*, 2022. 7

[55] Chao-Yuan Wu, Yanghao Li, Karttikeya Mangalam, Haoqi Fan, Bo Xiong, Jitendra Malik, and Christoph Feichtenhofer. Memvit: Memory-augmented multiscale vision transformer for efficient long-term video recognition. In *Proceedings of the IEEE/CVF Conference on Computer Vision and Pattern Recognition*, pages 13587–13597, 2022. 3

[56] Haoning Wu, Dongxu Li, Bei Chen, and Junnan Li. Longvideobench: A benchmark for long-context interleaved video-language understanding. *arXiv preprint arXiv:2407.15754*, 2024. 1

[57] Weijia Wu, Yuzhong Zhao, Zhuang Li, Jiahong Li, Hong Zhou, Mike Zheng Shou, and Xiang Bai. A large crossmodal video retrieval dataset with reading comprehension. *Pattern Recognition*, 157:110818, 2025. 5

[58] Junbin Xiao, Xindi Shang, Angela Yao, and Tat-Seng Chua. Next-qa: Next phase of question-answering to explaining temporal actions. In *Proceedings of the IEEE/CVF conference on computer vision and pattern recognition*, pages 9777–9786, 2021. 5, 6

[59] Junbin Xiao, Angela Yao, Zhiyuan Liu, Yicong Li, Wei Ji, and Tat-Seng Chua. Video as conditional graph hierarchy for multi-granular question answering. In *Proceedings of the AAAI Conference on Artificial Intelligence*, volume 36, pages 2804–2812, 2022. 7

[60] Dejing Xu, Zhou Zhao, Jun Xiao, Fei Wu, Hanwang Zhang, Xiangnan He, and Yueting Zhuang. Video question answering via gradually refined attention over appearance and motion. In *Proceedings of the 25th ACM international conference on Multimedia*, pages 1645–1653, 2017. 6

[61] Haiyang Xu, Qinghao Ye, Ming Yan, Yaya Shi, Jiabo Ye, Yuanhong Xu, Chenliang Li, Bin Bi, Qi Qian, Wei Wang, et al. mplug-2: A modularized multi-modal foundation model across text, image and video. In *International Conference on Machine Learning*, pages 38728–38748. PMLR, 2023. 7

[62] Mingze Xu, Mingfei Gao, Zhe Gan, Hong-You Chen, Zhengfeng Lai, Haiming Gang, Kai Kang, and Afshin Dehghan. Slowfast-llava: A strong training-free baseline for video large language models. *arXiv preprint arXiv:2407.15841*, 2024. 1

[63] Shen Yan, Tao Zhu, Zirui Wang, Yuan Cao, Mi Zhang, Soham Ghosh, Yonghui Wu, and Jiahui Yu. Videococa: Video-text modeling with zero-shot transfer from contrastive captioners. *arXiv preprint arXiv:2212.04979*, 2022. 7

[64] Antoine Yang, Antoine Miech, Josef Sivic, Ivan Laptev, and Cordelia Schmid. Just ask: Learning to answer questions from millions of narrated videos. In *Proceedings of the IEEE/CVF international conference on computer vision*, pages 1686–1697, 2021. 7

[65] Antoine Yang, Antoine Miech, Josef Sivic, Ivan Laptev, and Cordelia Schmid. Zero-shot video question answering via frozen bidirectional language models. *Advances in Neural Information Processing Systems*, 35:124–141, 2022. 7

[66] Zongxin Yang, Guikun Chen, Xiaodi Li, Wenguan Wang, and Yi Yang. Doraemongpt: Toward understanding dynamic scenes with large language models. *arXiv preprint arXiv:2401.08392*, 2024. 3

[67] Qinghao Ye, Guohai Xu, Ming Yan, Haiyang Xu, Qi Qian, Ji Zhang, and Fei Huang. Hitea: Hierarchical temporal-aware video-language pre-training. In *Proceedings of the IEEE/CVF International Conference on Computer Vision*, pages 15405–15416, 2023. 7

[68] Kexin Yi, Chuang Gan, Yunzhu Li, Pushmeet Kohli, Jiajun Wu, Antonio Torralba, and Joshua B Tenenbaum. Clevrer: Collision events for video representation and reasoning. *arXiv preprint arXiv:1910.01442*, 2019. 5

[69] Shoubin Yu, Jaemin Cho, Prateek Yadav, and Mohit Bansal. Self-chained image-language model for video localization and question answering. *Advances in Neural Information Processing Systems*, 36, 2024. 7

[70] Zhou Yu, Dejing Xu, Jun Yu, Ting Yu, Zhou Zhao, Yueting Zhuang, and Dacheng Tao. Activitynet-qa: A dataset for understanding complex web videos via question answering. In *Proceedings of the AAAI Conference on Artificial Intelligence*, volume 33, pages 9127–9134, 2019. 6

[71] Hang Zhang, Xin Li, and Lidong Bing. Video-llama: An instruction-tuned audio-visual language model for video understanding. *arXiv preprint arXiv:2306.02858*, 2023. 1, 2, 3, 4

[72] Xingyi Zhou, Anurag Arnab, Shyamal Buch, Shen Yan, Austin Myers, Xuehan Xiong, Arsha Nagrani, and Cordelia Schmid. Streaming dense video captioning. In *Proceedings of the IEEE/CVF Conference on Computer Vision and Pattern Recognition*, pages 18243–18252, 2024. 3

[73] Deyao Zhu, Jun Chen, Xiaoqian Shen, Xiang Li, and Mohamed Elhoseiny. Minigpt-4: Enhancing vision-language understanding with advanced large language models. *arXiv preprint arXiv:2304.10592*, 2023. 3